Available online at www.sciencedirect.com
SCIENCE DIRECT
Experimental Thermal and Fluid Science 30 (2006) 829–836
Experimental Thermal and Fluid Science
www.elsevier.com/locate/etfs

Explosive vaporization in microenclosures

G. Romera-Guereca [a,*], J. Lichtenberg [b], A. Hierlemann [b], D. Poulikakos [a], B. Kang [c]

[a] Laboratory of Thermodynamics in Emerging Technologies, ETH Zurich, CH-8092 Zurich, Switzerland
[b] Physical Electronics Laboratory, ETH Zurich, CH-8093 Zurich, Switzerland
[c] Department of Mechanical Systems Engineering, Chonnam National University, Gwangju, Republic of Korea

Abstract

The explosive vaporization of a liquid above planar microheaters induces a fast increase of pressure that is exploited in many thermally driven actuators in MEMS components such as ink jet printer cartridges, pumps, valves and optical switches. Some of these components need to enclose the working fluid as it is the case of valves in which the heated liquid is separated from the flow that it regulates by a flexible membrane. To achieve a better insight into the thermodynamic processes involved, the present work investigates experimentally an enclosed microsystem designed and fabricated for this purpose, composed of a small liquid volume (8 nL) heated by a electric pulse for 2 μs supplied to a planar microfabricated heater. During the heating, the temperature-induced change in resistance can be determined by imposing a defined current and measuring the voltage drop over the heater. While the chip is based on a silicon substrate with integrated platinum heaters and sensors, the structure enclosing the fluid (cavity and fluidic access to it) is made of a silicone elastomer, poly(dimethylsiloxane) (PDMS). This transparent material is widely used in microfluidics and allows for flexible and transparent walls that can be deflected by increasing the pressure inside the cavity. To seal the system the inlet and the outlet were closed by blocking them with a metallic stab. In the present work we visualize vaporization of isopropanol in contact with a suddenly heated planar resistor for two different cavity heights, 150 μm and 16 μm. The rate of temperature rise of the thin liquid layer in contact with the heater is of the order of 10^7 K s^{-1} for a pulse duration of 2 μs. We compare bubble growth and collapse for the open and closed systems. Compared to the open system, the bubble growth in the closed system is considerably damped.
© 2006 Elsevier Inc. All rights reserved.

Keywords: Explosive vaporization; Thermal bubble; Microenclosure; Microheater

1. Introduction

Since the thermal bubble technology has been successfully applied to eject ink droplets in ink jet printing in the early 1970s, researchers have shown increasing interest in bubbles generated by planar microheaters. This technology is based on the heat generated by an electrical current passing through a thin resistive element (Joule effect). When the heater is surrounded by a liquid, a thin layer of the liquid in contact with it reaches a very high temperature in a very short time and it may vaporize explosively. When this occurs the surface of the bubble compresses the surrounding liquid in a piston like effect. This effect may be used to produce mechanical work (microactuator). Some of the main advantages of this technology are: the absence of moving parts, high reproducibility with smooth expansion and recovering [1] and simple electric control.

The very fast development of MEMS is increasing the applicability of the thermally activated microactuators. This trend is specially noticeable in the field of microfluidic devices where chemical analysis may profit enormously from miniaturization [2]. For chemical and biochemical micro reactors movement and control of fluids and particles in fluids on the microscale is critical [3] and many designs of microvalves and micropumps include thermal bubbles as actuator mechanism [4]. The thermal bubble has been also proposed to improve mixing for microreactors [5] and as microinjector mechanism to improve fuel injection in internal combustion engines [6]. In some of

* Corresponding author.
E-mail address: gloria.romera@ethz.ch (G. Romera-Guereca).

0894-1777/$ - see front matter © 2006 Elsevier Inc. All rights reserved.
doi:10.1016/j.expthermflusci.2006.03.012

those systems the heater can be initially at ambient pressure but the developing bubble will generate a pressure pulse that may affect the onset and/or growth of the bubble. It seems that most of the applications will require a small enclosure surrounding the heater and our interest goes into understanding how confinement may affect vaporization. To the best of our knowledge, explosive vaporization of an enclosed liquid has not yet been sufficiently explored. In the literature we can only note the analysis of Van P. Carey [7]. In his investigation, Van P. Carey focuses on a liquid enclosed in a cavity with a flexible wall as in a typical microvalve. He uses the Redlich–Kwong equation of state and the principles of thermodynamics to calculate the spinoidals and saturation points of FC 72 and FC 75. His analysis predicts that a confinement of the liquid being heated increases the boiling temperature and it may inhibit spontaneous boiling. Another interesting approach is the theoretical work of Zhang et al. [8]. They study nucleation in microchannels and explore the concept of ''evaporation space''. This is defined as the minimum liquid bulk size required for bubble growth and it was first observed experimentally by Peng et al. [9].

In order to have reproducible explosive vaporization it is necessary to apply a very high heat flux to the liquid [10] so that the fluid reaches temperatures close to the theoretical expected superheat limit. Large gradients of temperature appear in the liquid close the hot surface. Rapid heating was first achieved by pulse heating of a wire immersed in a pool of fluid [11]. Thin metallic films have also been used for this purpose and researchers agree [12,13] that thin film heaters may be more suitable than wires to study bubble formation because they have lower thermal mass and practically defectless surfaces. Measuring the temperature of the liquid layer in contact with the heater is not a trivial problem due to the high speed of the phenomena to be observed and the small dimensions at hand. Within a good approximation this temperature is assumed to be the same as that of the contact surface. For planar or wire resistances under pulse heating, the temperature of the heater can be determined non-intrusively by measuring the change in electrical resistance [14]. This method allows for monitoring the change in average temperature of the resistor during the heating process. Of special scientific interest is to determine the temperature at the moment when vaporization starts (boiling incipience). In general the closer the boiling incipience temperature to the spinodal temperature is, the higher the probability to have homogeneous nucleation and thus more reproducible phenomena. Also, the closer to the spinodal the more explosive will the phenomena be. Boiling incipience can be detected by determining the inflection point in the temperature evolution curve. This method is described in detail in [14] for commercial tantalum–aluminum heaters. In the aforementioned work, the experiments showed good qualitative agreement with homogenous nucleation theory for high heating rate experiments. Other researchers could not observe such an inflection in the temperature evolution curve and had to rely on visualization results to find the boiling incipience temperature. This is the case of the work by Iida et al. [15] who used fine time resolved visualization of the initial stage of heating to study the incipience of boiling. They conclude that the temperature at the boiling incipience increases with the increase of the rate of temperature rise and approaches the homogenous nucleation temperature for ethyl alcohol and toluene. For water, the maximum boiling incipience temperature measured was about 20 °C below the value predicted by homogenous nucleation theory.

Together with boiling incipience the growth of the bubble during and after applying the heating pulse has also been investigated. Assai proposes a model for nucleation and bubble dynamics showing also the experimental results matching his models [10,16]. He explains the phenomena defining different regimes, first nucleation in the superheated liquid then instantaneous formation of a vapor film followed by rapid bubble growth due to the pressure impulse, and bubble collapse.

The effect of ambient pressure has been assessed by Pavlov and Skripov [11] and later by Derwnicki [17]. The later presented experimental results of a heated platinum wire immersed in a pressurized chamber full of water. Iida et al. [12] studied the effect of ambient pressure on pool boiling of ethyl alcohol heated by a planar platinum heater. Their experiments were performed inside a pressurized chamber with a transparent window facing the objective of the microscope. The pressure wave originated by the expanding bubble generated by a commercial heater actuated inside a pool of liquid was measured by Glod et al. [18] using a microphone located 1 mm from the source.

In our work we will impose a rate of temperature rise of the order of 10^7 K s^{-1} to a planar platinum microheater. We measure the average temperature on the heater and visualize the boiling inside a microcavity made of a transparent flexible polymer widely used in microfluidics devices. Our goal is to determine how confinement affects explosive vaporization and which parameters may be of interest when designing microactuators based on the ''thermal bubble'' principle.

2. Microfabrication overview

Square, planar platinum heaters of 100 μm side length have been fabricated on two different substrates: (a) 300 μm thick silicon wafer with a 1.5 μm thick layer of thermally grown silicon dioxide, and (b) 500 μm thick Pyrex wafer. The fabrication follows conventional photolithographic and thin-film processing: After cleaning of the wafer, Microposit 1828 positive resist (Shipley, USA) was patterned for metal lift-off and the possible photoresist residues were removed in oxygen plasma. Then, 5 nm chromium was deposited by sputtering as adhesion layer followed by a 100-nm platinum layer. The metal layer is subsequently patterned by removing the underlying photoresist in acetone (lift-off). After a second cleaning step, a 200-nm-thick layer of silicon nitride is deposited as protec-

tive, insulating layer by plasma-enhanced chemical vapor deposition (PECVD). Microposit 1828 is patterned on the silicon nitride before opening the nitride layer for electric contacts using reactive-ion etching (RIE). To finalize the processing of the heater chip, the remaining photoresist is dissolved. Fig. 1 is a microphotograph of the heater device: The heater (100×100 μm^2) is in the middle of the image. Two connections for voltage-drop measurement (voltage taps) are located in top left corner and bottom right corner of the heaters. Large electric contacts to supply the heating pulse extend out of the image. Two conductive electrodes, and an auxiliary temperature sensor were included in the design. The auxiliary temperature sensor is a meander shape resistor. It is used to control the temperature of the substrate.

The microfluidic cavity (Fig. 2) with an inlet and an outlet is made by micromolding of a layer of poly(dimethyl siloxane) (PDMS) of a controlled thickness using a mold made of SU8 (photostructurable, epoxy-based resist, Microchem, USA). The mold is fabricated on a silicon wafer, which is cleaned first, followed by spin-coating of SU-8 50 and soft baking. Then, the resist is exposed through a mask with the shape of the cavity and channels, and post-exposure baked to cross-link the resin. After developing, the resulting polymer structures on the master are about 150 μm high. Then, a degassed mixture of PDMS prepolymer and cross-linking agent is poured onto the master and cured at 65 °C for 4 h on a hot plate. The PDMS is subsequently peeled off. Fluidic access into the cavity is provided by punching holes into the cured PDMS layer prior to bonding. The cavity is aligned to the heater and bonded.

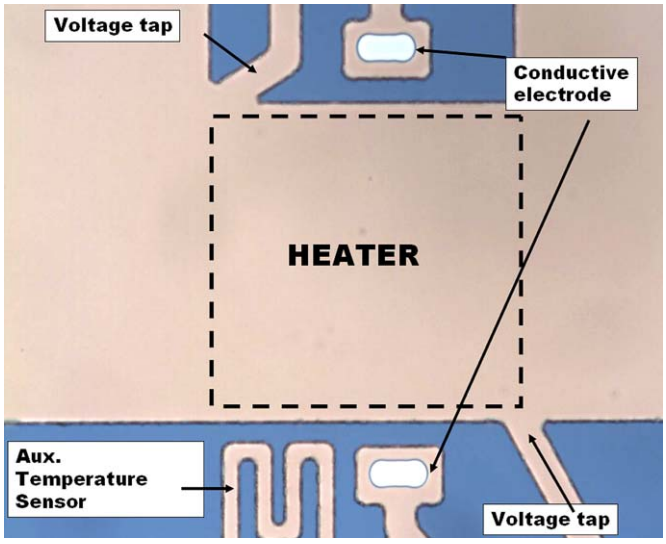

Fig. 1. Photograph of the microfabricated heater. The heater (100×100 μm^2) is in the middle. Large electric contacts to supply the heating pulse extend out of the image. Two additional thin electrical connections for voltage-drop measurement (voltage taps) are located at top left corner and bottom right corner of the heaters to allow 4 points resistivity measurement. The meander shape resistor bottom left is used as auxiliary temperature sensor to control substrate temperature. The two electrodes located both sides of the heater are used as conductivity sensor.

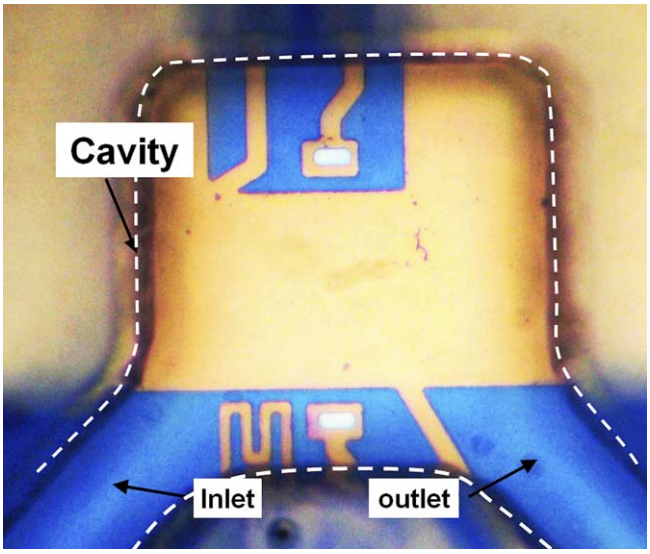

Fig. 2. Photograph of the assembled chip. The heater (100×100 μm^2) is in the middle and the two connections for voltage-drop measurement (voltage taps) are in the centre. The bigger square marked with dashed line is the top view of the cavity, (200 μm side square). The channels to fill the cavity with liquid are 50 μm wide and several millimetres long so that the inlet/outlet (out of the image) can be accessed when the device is under the microscope.

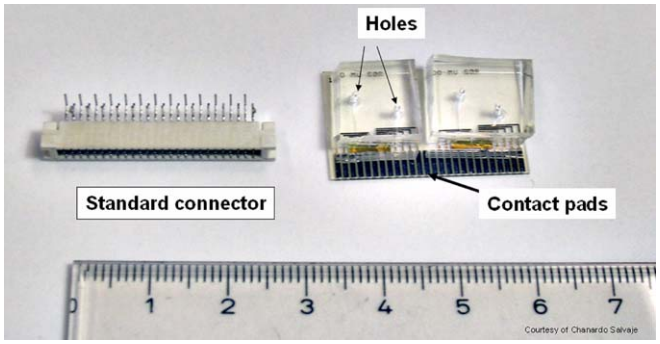

Fig. 3. Assembled chip consisting on two test devices (right) and a standard connector used to simplify the electrical connection (left). Holes to access the fluidic channels are punched onto the PDMS cover prior to bonding.

To facilitate packaging, all electrical connections were placed at one side of the chip so as to match the contacts of a standard flat-cable connector (Flexprint connectors, Amphenol, 26 contacts). Fig. 3 shows the standard connector, (left), and the assembled chip with two test devices, (right). The connector can be soldered to an external circuit board and fixed onto the microscope stage. The chip can be easily replaced.

3. Experimental set-up

The experimental set-up is shown in Fig. 4. The device is placed on a circuit board fixed to the stage of an Olympus

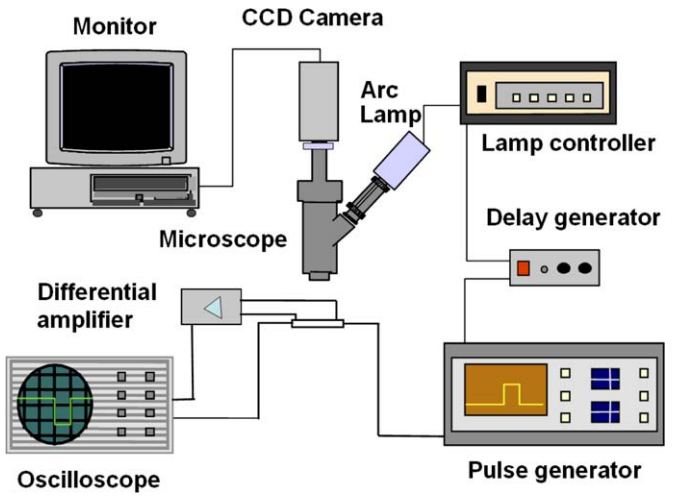

Fig. 4. The set-up consists of a video microscope with a synchronized arc lamp for stroboscopic monitoring. A delay unit triggers the current pulse generator and the lamp. The electrical current passing by the heater and the voltage drop are acquired using an oscilloscope.

BX40 microscope. To produce bubbles a current pulse is supplied to the planar heater. This heating pulse, is of about 1 A and 4 μs duration and is provided by a pulse generator (HP B114A). Resistive temperature measurement is simultaneously performed using as temperature sensor the heater itself. The voltage drop over the heater is picked up by two voltage taps, which are connected to a differential amplifier (LeCroy DA1822) and monitored using a storage oscilloscope (LeCroy LC334 A). The current supplied to the heater through the wider electrical connections is also monitored using an APO15 current probe (LeCroy). This 4 point configuration for the measurement of the resistance change reduces measurement errors. The instantaneous electrical resistance of the heater $R(t)$, is obtained by dividing the measured voltage difference $V(t)$ by the monitored current $I(t)$:

$$R(t) = V(t)/I(t)$$

The change in resistance of the heater is related to the change in temperature:

$$R = R_0\,(1 + \alpha\Delta T)$$

where R_0 is the nominal resistance measured at the reference temperature and α is the temperature coefficient of resistance. The temperature during cooling down phase can be measured by setting a low level value for the electrical current pulse. When working with volatile liquids as isopropanol this constant current may accelerate the evaporation of the liquid affecting the repeatability of the experiment. We did not measure temperature during cooling down phase for the experiments presented here.

In order to visualize the vaporization, an arc-lamp is used as light source, each flash being synchronized with the heating pulse. A CCD camera is mounted on the microscope and connected to a computer-controlled frame grabber. A home-made pulse-delay unit generates triggering signals for both, the pulse generator and the lamp [19]. The delay between the heating pulse and the arc-lamp can be tuned to visualize different points in time during the process. Tuning the pulse delay allows the acquisition of a sequence of images.

3.1. Heater calibration

The heater has been calibrated measuring the resistance at different temperatures using a four-wire technique. To this end a test device specially designed for calibration purposes and fabricated on the same wafer as the heaters is placed inside an oven, (Thermolyne Furnace 1300) and its resistance is measured by a data acquisition unit HP 3852A connected to a PC. The temperature coefficient of resistance (α) measured for the fabricated devices is $2.0 \times 10^{-3}\ \mathrm{K}^{-1}$. No drift due to thermal cycling has been found.

4. Results

For each test-run the current intensity and voltage drop are recorded. Typical traces are shown in Fig. 5. A current pulse of intensity in the range 1–1.3 A is supplied to the heater. Below this amplitude range the vapor layer formed due to the convergence of nucleation sites covers only partially the heater. Fig. 6 shows the average temperature vs. time. The origin of abscissas is the onset of the heating pulse. We use the temperature evolution curve to determine the rate of temperature rise. An increase of the current amplitude increases the rate of temperature rise. Using isopropanol as the working fluid, a rate of temperature rise of $10^7\ \mathrm{K\ s^{-1}}$ has been obtained. To avoid rapid deterioration of the heater we set the pulse length so that the heating stops immediately after having a vapor layer covering the entire heater area.

Vaporization sites appear first in the region close to the heater corners. These regions seam to be the hottest area on the heater due to a non-uniform electrical current intensity distribution induced by the asymmetric heater layout. This initial vapor region grows by merging to adjacent vaporization sites toward the colder area of the heater. At the moment the pulse is stopped the vapor region covers the

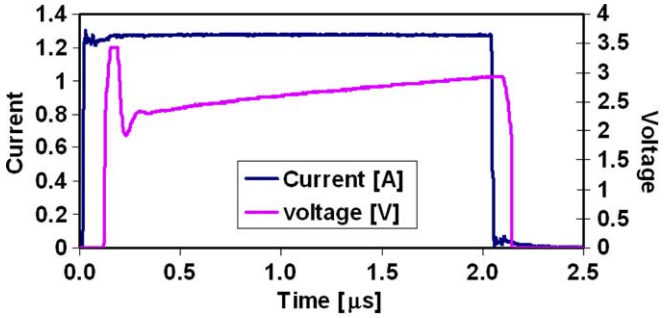

Fig. 5. Typical current and voltage traces.

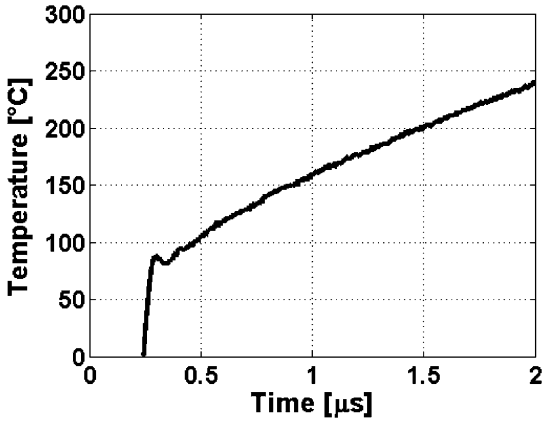

Fig. 6. Average temperature on the heater for a test-run. The heating rate is 10^7 K s^{-1} (Isoporopanol).

entire heater. Then, the vapor layer grows in the direction perpendicular to the wall and then it starts to collapse. In general, the current intensity and the pulse duration determine the extent of the region covered with vapor on the heater.

We present the results obtained with a high heating rate. The vaporization sequence shown in Fig. 7 corresponds to vaporization of isopropanol when the inlet and the outlet are open to the ambient. A pulse of 1.3 A lasting 2 μs. has been applied. The heating pulse stops immediately after the heater surface is covered with vapor. In the first frame in Fig. 7, taken 1 μs after turning on the heating pulse, it can be seen that vapor bubbles form first at the corners close to the voltage taps. The appearance of a layer of vapor covering the heater is evident in the second image (2 μs). The heater is almost completely covered by a vapor layer with an irregular bubble boundary, due to individual growth of nuclei surface, as it has been identified by other authors [10]. The heating pulse is turned off in this case after 2 μs. The bubble grows from this layer (inertial growth) in the direction perpendicular to the heater surface, and in the fifth image, (5 μs) it can be seen that it starts to shrink and it collapses entirely within 11 μs.

The same heater was used to record a second set of images imposing the same current. In this case the inlet and the outlet were closed by blocking them with a 1 mm

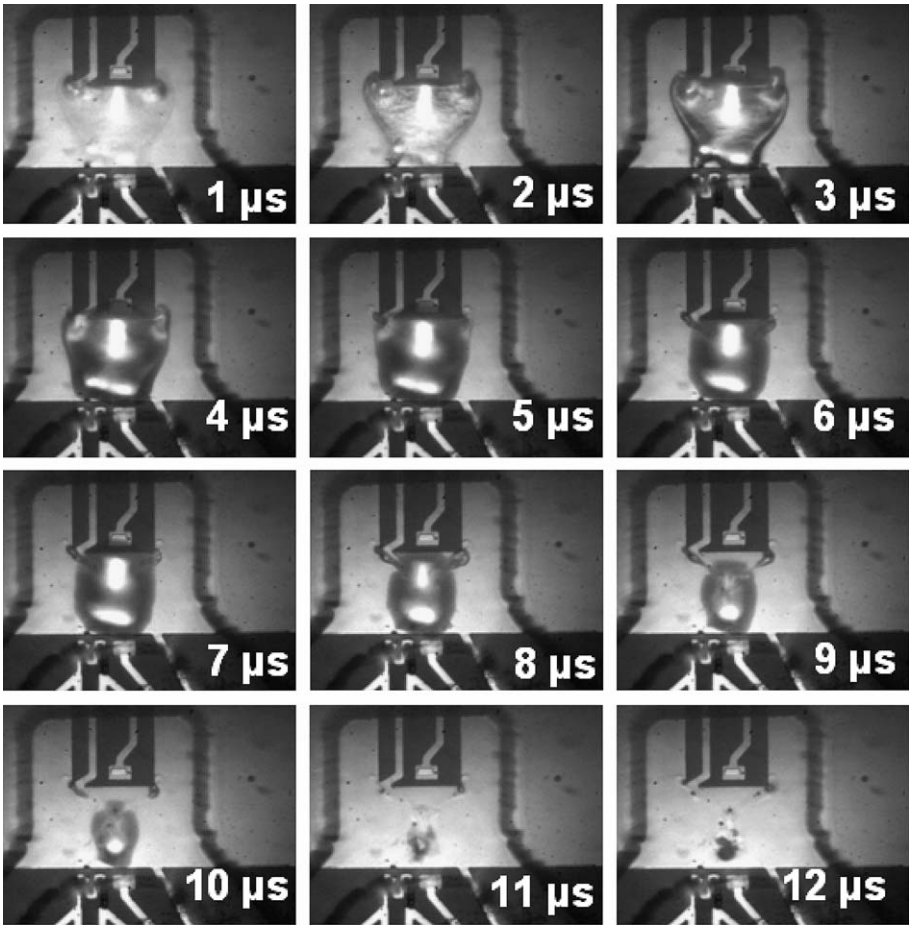

Fig. 7. Sequence of images showing explosive vaporization of isopropanol on a 100×100 μm^2 planar microheater. The liquid is confined by a square cavity 200 μm side and 150 μm high made of poly(dimethyl siloxane) (PDMS). The fluidic inlet and outlet to the cavity are let open to the ambient. Heating pulse supplied: 1.3 A and 2 μs.

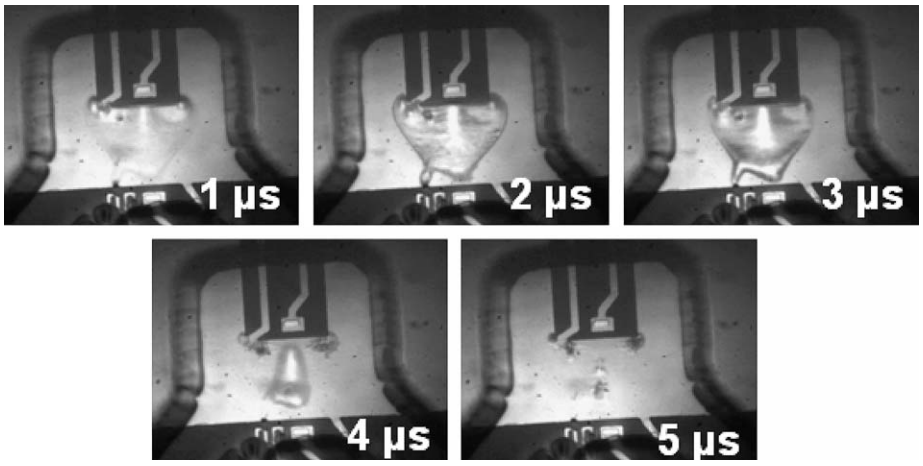

Fig. 8. Sequence of images showing the explosive vaporization of isopropanol on a $100 \times 100\ \mu m^2$ planar microheater. The liquid is confined by a square cavity 200 µm side and 150 µm high made of poly(dimethyl siloxane) (PDMS). The fluidic inlet and outlet to the cavity are tightly closed. Heating pulse supplied: 1.3 A and 2 µs.

diameter metallic stab. In order to avoid having air trapped into the system the stabs were introduced while keeping the chip within a container full of isopropanol. The sequence of images acquired for this test run is shown in Fig. 8. The first two images, corresponding to the formation of the vapor film are quite similar to the previous sequence. In the third image, corresponding to the 3 µs after turning on the heating pulse noticeable difference can be observed. The not so dark bubble perimeter suggests less growth in the direction perpendicular to the heater plane, as if further growth is damped by the increasing pressure developed inside the micro chamber.

In order to compare the two sets of microphotographs acquired, for the open (Fig. 7) and closed (Fig. 8) systems, the images have been further processed. For each image the bubble area projected on the heater surface divided by the heater surface area have been calculated and depicted against acquisition time. Results are shown in Fig. 9. The origin of time is set on the trigger of the heating pulse. The vertical line indicates the pulse duration. It can be seen that there is a rapid increase of the bubble projected area at the initial stage and that the closed system shows a slightly smaller maximum bubble projected area. The bubble collapsing stage is longer for the open system with a total bubble life time of 10 µs, 5 µs longer than that for the closed system.

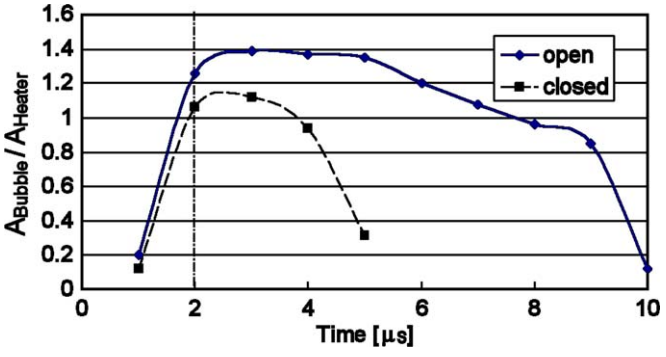

Fig. 9. Bubble surface area projected on the heater surface divided by the heater surface as a function of time for open and closed systems with a cavity height of 150 µm. Heating pulse supplied: 1.3 A and 2 µs. Each data point is obtained by processing a microphotograph taken during a single run. The time in µs represented in the x axis is the delay between leading edge of the heating pulse and flash lamp shot. The images used to calculate this data points are depicted in Fig. 7 for the open system, and Fig. 8 for the closed system.

In the previous experiments the PDMS cavity is about 150 µm high. Experiments have been also performed using a cavity only 16 µm in height. The next visualization set, (Fig. 10), shows a sequence of images taken for a pulse of 1.14 A and 2.3 µs. Vaporization initiates already in the first image of the set, corresponding to 1 µs. The bubble projected area extends as long as the heating pulse is on and then it is maintained while the bubble grows in the direction perpendicular to the plane. The bubble starts to shrink in the fifth image corresponding to 5 µs after turning on the heating pulse. The bubble collapses approximately 10 µs after turning on the heating pulse, with a total life time of 10 µs similar to the first case presented. Also for this set of tests the closed system has been studied. The sequence shows no marked difference in the growth pattern, and it has only about 1 µs shorter lifetime. The effect of the height of the fluidic cavity will be explored carefully in the future before definitive statements on its effect can be made.

The similarity between the open and closed systems in the case of shallow cavity is maybe due to the fact that the growth in the perpendicular direction is already inhibited by the top wall in the open case as well. We expect also the thickness of the PDMS above the cavity to play an important role in the phenomena, as it modifies the flexibility of the wall above the heater. This parameter could not be controlled in the present experiments, but we intend to study this effect in future works.

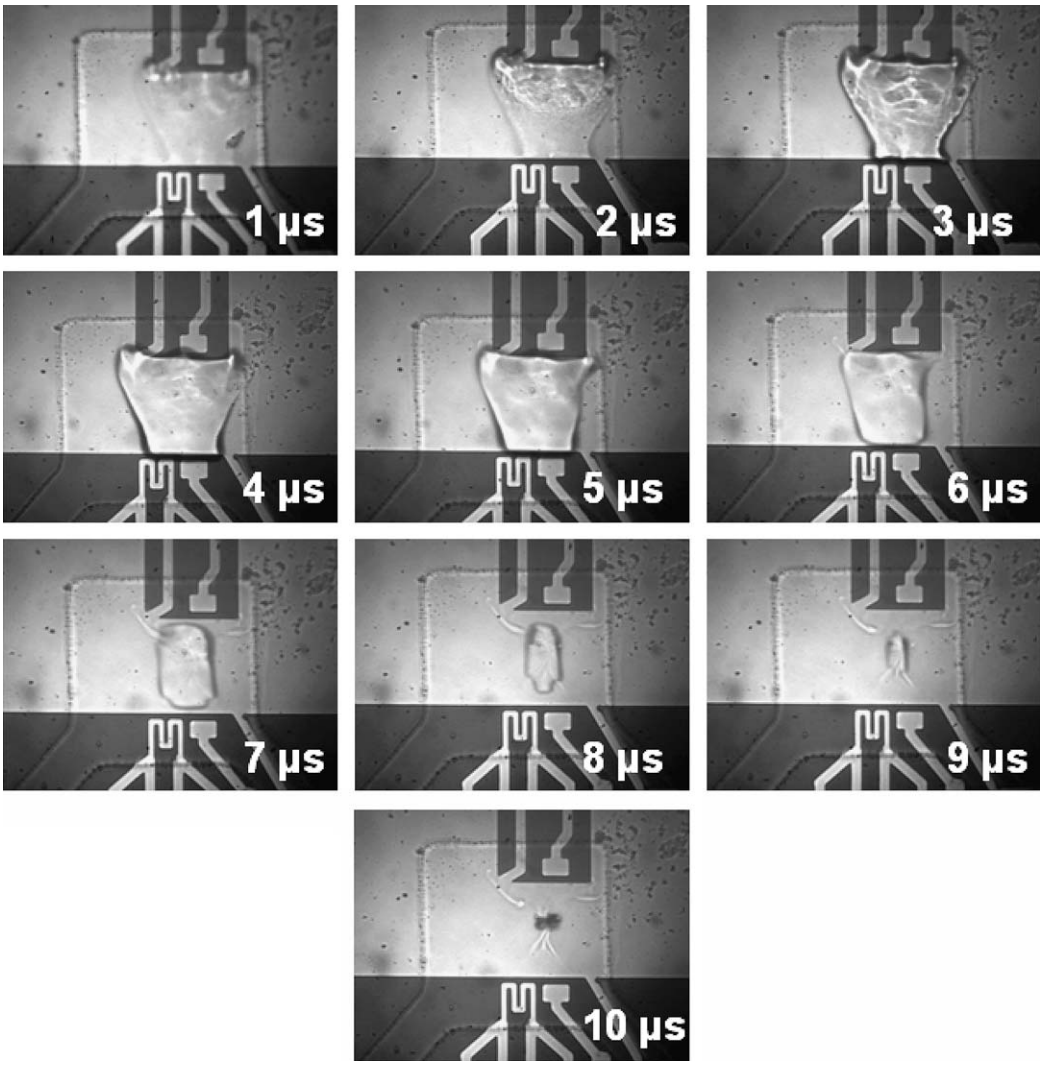

Fig. 10. Sequence of images showing explosive vaporization of isopropanol on a 100×100 μm^2 planar microheater. The liquid is confined by a square cavity 200 μm side and 16 μm high made of poly(dimethyl siloxane) (PDMS). The fluidic inlet and outlet to the cavity are left open to the ambient. Heating pulse supplied: 1.14 A and 2.3 μs.

5. Conclusions

A test device has been fabricated using standard micro fabrication technologies and a simple packaging solution for both electronic and fluidic parts. PDMS has been successfully combined with silicon technology in order to obtain a flexible and transparent fluidic chamber. This concept seems to be a promising research tool allowing experiments in confined systems.

A reliable set-up for heating pulse generation and signal readout has been used to visualize bubble formation inside a flexible cavity. A rate of temperature rise of the order of 10^7 K s^{-1} has been achieved.

Based on the observations in a confined system the bubble growth may be strongly damped by the confinement and this should be considered for design purposes. No significant effect on the onset of vaporization has been observed up to now but this may be due to an excess of dead volume in the system and/or the mechanical characteristics of PDMS. Future work will aim at resolving these and other thermofluidic issues for the microsystem under study.

Acknowledgements

This work is being supported by the Swiss National Science Foundation under grant number 2000-067738/1 and by the Korea Research Foundation Grant KRF-2003-013-D00014.

References

[1] K. Okuyama, S. Tsukahara, N. Morita, Y. Iida, Transient behavior of boiling bubbles generated on the small heater of a thermal ink jet printhead, Experimental Thermal and Fluid Science 28 (8) (2004) 825–834.

[2] A. Manz, N. Graber, H.M. Widmer, Miniaturized total chemical-analysis systems, Sensors and Actuators. B Chemical 1 (1–6) (1990) 244.

[3] R.B. Maxwell, A.L. Gerhardt, M. Toner, M.L. Gray, M.A. Schmidt, A microbubble-powered bioparticle actuator, Journal of Microelectromechanical Systems 12 (5) (2003) 630.
[4] Z. Yin, A. Prosperetti, A microfluidic 'blinking bubble' pump, Journal of Micromechanics and Microengineering 15 (3) (2005) 643–651.
[5] J.H. Tsai, L. Lin, Active microfluidic mixer and gas bubble filter driven by thermal bubble micropump, Sensors and Actuators A-Physical 97 (8) (2002) 665–671.
[6] Y.-K. Lee, U.-C. Yi, F.-G. Tseng, Fuel injection by a thermal microinjector, in: Proceedings of MEMS, ASME IMECE, 1999.
[7] V.P. Carey, Thermodynamic analysis of the intrinsic stability of superheated liquid in a micromechanical actuator with elastic walls, Microscale Thermophysical Engineering 4 (2) (2000) 109–123.
[8] J.T. Zhang, X.F. Peng, G.P. Peterson, Analysis of phase-change mechanisms in microchannels using cluster nucleation theory, Microscale Thermophysical Engineering 4 (2000) 177–187.
[9] X.F. Peng, B.-X. Wang, Forced convection and flow boiling heat transfer for liquid flowing through microchannels, International Journal of Heat and Mass Transfer 36 (14) (1993) 3421–3427.
[10] A. Asai, Bubble dynamics in boiling under high heat flux pulse heating, Journal of Heat Transfer 113 (1991) 973–979.
[11] P.A. Pavlov, V.P. Skripov, Kinetics of spontaneous nucleation in strongly heated liquids, High Temperature 8 (3) (1970) 540–545.
[12] Y. Iida, K. Okuyama, T. Endou, Boiling nucleation on a very small film heater subjected to extremely rapid heating – effect of ambient pressure on bubble formation by fluctuation nucleation, JSME International Journal Series B-Fluids and Thermal Engineering 40 (2) (1997) 250–256.
[13] L. Lin, Microscale thermal bubble formation: thermophysical phenomena and applications, Microscale Thermophysical Engineering 2 (1998) 71–85.
[14] C.T. Avedisian, W.S. Osborne, F.D. McLeod, C.M. Curley, Measuring bubble nucleation temperature on the surface of a rapidly heated thermal ink-jet heater immersed in a pool of water, Proceedings of the Royal Society of London Series A-Mathematical Physical and Engineering Sciences 455 (1991) (1999) 3875–3899.
[15] Y. Iida, K. Okuyama, K. Sakurai, Boiling nucleation on a very small film heater subjected to extremely rapid heating, International Journal of Heat and Mass Transfer 37 (17) (1994) 2771–2780.
[16] A. Asai, S. Hirasawa, I. Endo, Bubble generation mechanism in the bubble jet recording process, Journal of Imaging Technology 14 (5) (1988) 120–124.
[17] K.P. Derewnicki, Experimental studies of heat transfer and vapour formation in fast transient boiling, International Journal of Heat Mass Transfer 28 (11) (1985) 2085–2092.
[18] S. Glod, D. Poulikakos, Z. Zhao, G. Yadigaroglu, An investigation of microscale explosive vaporization of water on ultrathin Pt wire, International Journal of Heat and Mass Transfer 45 (2) (2002) 367–379.
[19] S. Glod, Explosive Vaporization of Water on Thin-Film Microheaters and Ultrathin Platinum Wires, Department of Mechanical and Process Engineering, Zurich, 2001.